Acta Oceanol. Sin., 2020, Vol. 39, No. 10, P. 11–26
https://doi.org/10.1007/s13131-020-1656-3
http://www.hyxb.org.cn
E-mail: hyxbe@263.net

Spatiotemporal variability of physical-biogeochemical processes and intrinsic correlations in the semi-enclosed South Yellow Sea

Qinsheng Wei[1, 2*], Baodong Wang[1, 2], Mingzhu Fu[1, 2], Junchuan Sun[1, 4], Qingzhen Yao[2, 3], Ming Xin[1], Zhigang Yu[2, 3]

[1] First Institute of Oceanography, Ministry of Natural Resources, Qingdao 266061, China

[2] Laboratory for Marine Ecology and Environmental Science, Pilot National Laboratory for Marine Science and Technology (Qingdao), Qingdao 266237, China

[3] Frontiers Science Center for Deep Ocean Multispheres and Earth System, Ministry of Education, Ocean University of China, Qingdao 266100, China

[4] Laboratory for Regional Oceanography and Numerical Modeling, Pilot National Laboratory for Marine Science and Technology (Qingdao), Qingdao 266237, China

Received 28 August 2019; accepted 19 March 2020

Abstract

Investigating the spatiotemporal variability of biogeochemical processes and ecological responses under multiple physical controls in shelf seas is of great importance for obtaining an in-depth understanding of marine ecosystem. Based on a compiled data set of historical observations and remote sensing data, the spatiotemporal variability and heterogeneity of physical-biogeochemical processes in the semi-enclosed South Yellow Sea (SYS) are investigated, and the intrinsic connectivity among different subregions and the associated mechanisms are examined. The results show that the seasonal alternation between southward transport in cold seasons and upwelling-induced vertical delivery in warm seasons is the primary physical control of the biogeochemical processes and primary production off Shidao and in the area adjacent to the Haizhou Bay. The northeastward expansion of coastal waters in the Subei Shoal constitutes an important physical driver for the offshore transport of *Ulva prolifera* in summer. Stratification significantly affects the biogeochemical processes in the Yellow Sea Cold Water Mass (YSCWM)-dominated area during warm seasons, and nutrients can accumulate in bottom waters from spring to autumn, making the Yellow Sea Cold Water Mass (YSCWM) be an important nutrient pool. Upwelling around the YSCWM boundary in the stratified season leads to consistency among the high chlorophyll *a* (Chl *a*) area, high primary productivity region and low-temperature upwelling zone. During cold seasons, the interactions of the southward cold waters in the western nearshore area and the northward warm waters in the central region lead to an "S"-shaped front in the SYS. In summer, upwelling can extract nutrients from the YSCWM; thus, the biogeochemical-ecological processes inside the cold-water mass and in the frontal zone are well connected via upwelling, and three typical physical-biogeochemical coupling regions are generated, namely, the Shidao coast, the area beyond the Haizhou Bay and the area off the Subei Shoal. This work refines and integrates studies on regional oceanography in the SYS and provides a comprehensive and systematic framework of physical-biogeochemical-ecological processes.

Key words: physical-biogeochemical process, upwelling, front, Yellow Sea Cold Water Mass, South Yellow Sea

Citation: Wei Qinsheng, Wang Baodong, Fu Mingzhu, Sun Junchuan, Yao Qingzhen, Xin Ming, Yu Zhigang. 2020. Spatiotemporal variability of physical-biogeochemical processes and intrinsic correlations in the semi-enclosed South Yellow Sea. Acta Oceanologica Sinica, 39(10): 11–26, doi: 10.1007/s13131-020-1656-3

1 Introduction

Continental marginal shelf seas are among the areas that experience intensive physical-biogeochemical interactions and can greatly contribute to the primary production of oceans (Gattuso et al., 1998; Simpson and Sharples, 2012). Investigating the spatiotemporal variability of biogeochemical processes and ecological responses beyond multiple physical controls in shelf seas is of great importance to obtain a comprehensive understanding of marine ecosystems. The Yellow Sea (YS), a typical semi-enclosed shelf sea of the northwest Pacific Ocean, is located between China's mainland and the Korean Peninsula (Fig. 1). The YS has curved shorelines and complex topography, and the line connecting Chengshantou on the Shandong Peninsula of China and Chang San-got in Korea divides the YS into two parts, the North Yellow Sea (NYS) and the South Yellow Sea (SYS). As a crucial region for the development of the marine-based economies of China and Korea, the YS is greatly influenced by human activities (Wang et al., 2015a; Khim et al., 2018). Moreover, the YS and

Foundation item: The National Key Research and Development Program of China under contract No. 2016YFC1402100; the National Natural Science Foundation of China under contract Nos U1906210 and 41876085; the Open Fund of the Laboratory for Marine Ecology and Environmental Science, the Qingdao National Laboratory for Marine Science and Technology under contract No. LMEES201808; the Basic Scientific Fund of the National Public Research Institutes of China under contract No. GY0220S03; the National Project of Comprehensive Investigation and Research of Coastal Seas in China under contract No. 908-01-ST03.
*Corresponding author, E-mail: weiqinsheng@fio.org.cn

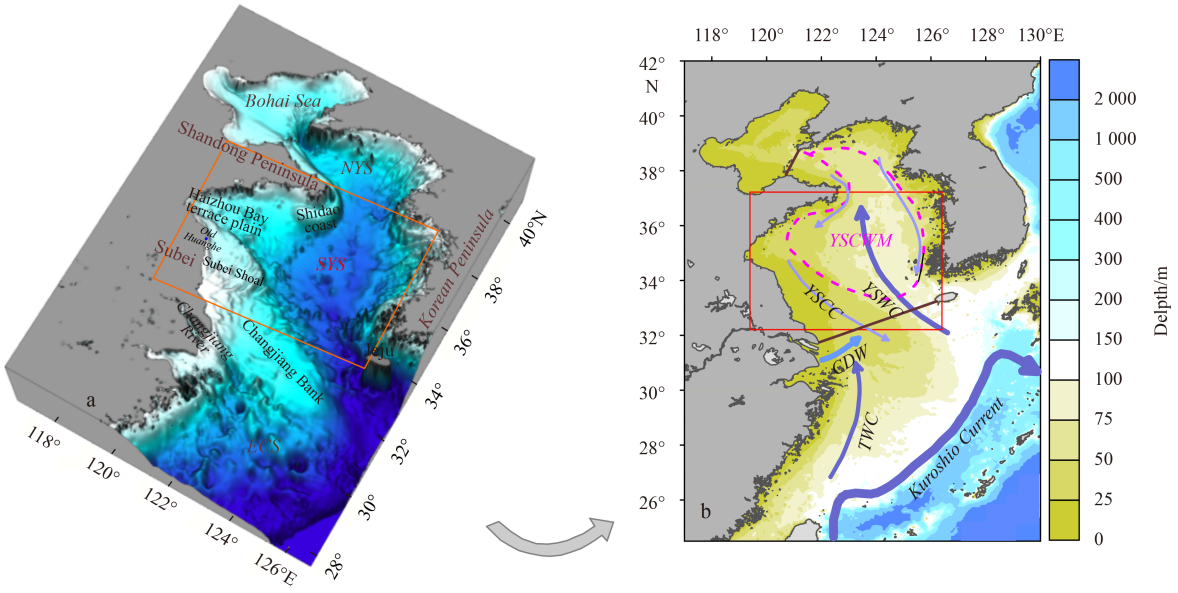

Fig. 1. Topography and general current fields in the SYS and adjacent sea areas. YSWC and YSCC represent the Yellow Sea Warm Current and Yellow Sea Coastal Current, respectively, in cold seasons; the dashed pink circle indicates the general location of the YSCWM in warm seasons; and TWC and CDW represent the Taiwan Warm Current and the Changjiang Diluted Water, respectively.

its adjacent East China Sea (ECS) are forced by the Kuroshio Current (i.e., the Pacific western boundary current) (Isobe, 2008; Wang and Oey, 2016) and the East Asian monsoon, which typically results in a prevailing stronger northerly wind in winter and weaker southerly wind in summer. Due to its high biological diversity and complicated food web structure, the YS is one of the most important Large Marine Ecosystems in the world (Tang et al., 2016).

The SYS has properties of a semi-closed system and an open system (Fig. 1). The circulations in this region and adjacent seas present significant spatiotemporal variations. In the central SYS, the Yellow Sea Cold Water Mass (YSCWM) is the primary physical process in the bottom layer during summer (Ho et al., 1959; Zhang et al., 2008; Wei et al., 2015; Li et al., 2016; Yuan et al., 2017), greatly influencing the hydrography, material transport and biogeochemical cycles of the YS, and a frontal zone is present at the boundary of the YSCWM (Zhao, 1987; Lü et al., 2010; Ren et al., 2014). In winter, the saline Yellow Sea Warm Current (YSWC) intrudes into the central SYS from southwest of Jeju Island (Lie et al., 2009, 2019; Huang et al., 2010; Lin et al., 2011; Liu et al., 2015a; Lie and Cho, 2016), interacting with the southward Yellow Sea Coastal Current (YSCC) and, together with the YSCC, affecting the water exchange and material transport in the YS and its adjacent ECS (Guo et al., 2003; Yuan et al., 2008; Chen, 2009; Bian et al., 2013; Wei et al., 2016b). Notably, seasonal alternations between the YSCWM and the YSWC occur in the central SYS. The remnant YSWC waters from cold seasons provide a significant background for the formation of the YSCWM during warm seasons (Ho et al., 1959; Yu et al., 2006; Wei et al., 2013d).

Several other specific subareas/geographical units exist in the SYS (Fig. 1). The Subei Shoal, which is located in the western part of the SYS, is dominated by a shallow topography that extends pinnately toward the southeast and northeast. The area northeast of the shoal is characterized by a pronounced topographic gradient. The area southeast of the Subei Shoal is connected to the Changjiang Bank, generating a large tongue-shaped shoal that spreads southeastward. The southern part of this shoal is an underwater valley oriented from southeast to northwest (Fig. 1), through which the northward Taiwan Warm Current (TWC) flows to the Changjiang River Estuary and the area southwest of the SYS underneath the Changjiang Diluted Water (CDW) plume. North of the Subei Shoal is the Haizhou Bay terrace plain, where the terrain deepens from west to east/southeast. The outer edge of this terrace plain connects with the central SYS. The shorelines in the region north of the Haizhou Bay and south of the Shandong Peninsula are typically oriented from southwest to northeast; notably, this region is steeper than the Subei Shoal. The Shidao coast to the east of the Shandong Peninsula is the pathway of the YSCC from the NYS to the SYS during cold seasons. This area is also adjacent to the Shidao fishing ground, which is one of the most important fisheries in the YS.

Variable hydrographic conditions and complicated geographic features highlight the complexity of the ecosystem dynamics in the SYS. Previous studies have been conducted on the physical/biogeochemical/ecological processes in the central YSCWM area (Wang, 2000; Zhang et al., 2008; Sun et al., 2013; Wei et al., 2013a; Yuan et al., 2014; Liu et al., 2015b; Shi et al., 2017; Fu et al., 2018) and in the boundary frontal zone of the YSCWM (Zhao, 1985, 1987; Lie, 1986; Wei et al., 2003; Zhou et al., 2008; Wei et al., 2010b, 2016a; Lü et al., 2010; Liu et al., 2015c). However, there are few investigations on the physical-biogeochemical features and ecological responses in other subregions of the SYS, such as the Shidao coast, the Subei Shoal and Haizhou Bay. Moreover, a systematic understanding of biogeochemical processes beyond the dual-drivers of seasonal stratification (Wei et al., 2002; Qiao et al., 2004; Bai et al., 2004) and frontal system (Zhao, 1987; Lü et al., 2010) in the YSCWM area is also lacking. Furthermore, the intrinsic connectivity and mechanisms of the hydro-biogeochemical processes in different subregions of the SYS from a systematic/comprehensive perspective are seldom analyzed.

In this paper, based on a combination of remote sensing data and integrated historical observations, we investigate the spatiotemporal variability and heterogeneity of the physical-biogeo-

chemical processes in the SYS and examine their intrinsic correlations and associated mechanisms from new insights. The purpose of this study is to further refine, integrate and promote research of oceanographic processes in the SYS to achieve a comprehensive and systematic understanding of this subject, thereby providing a scientific basis for the depiction of biogeochemical dynamics, construction of regional models, and establishment of ecological simulations in the YS Large Marine Ecosystem.

2 Data sources and methods

In this study, the satellite-derived climatological monthly mean SST (sea-surface temperature) data (during 1982–2008) of the SYS were obtained from the National Oceanic and Atmospheric Administration's (NOAA's) National Climatic Data Center (https://data.nodc.noaa.gov/pathfinder/Version5.0_Climatologies/1982_2008/Monthly/). The climatological monthly mean SSTs in February and August correspond to winter and summer, respectively.

The compiled shipboard data were primarily obtained from seasonal surveys during 2006–2007 under the special project "Comprehensive Survey and Evaluation of Coastal Seas of China", generally including data from April 2007 (spring), July 2006 (summer), October 2007 (autumn) and January 2007 (winter). The adopted parameters comprised temperature, salinity, density, nutrients, suspended particulate matter (SPM), chlorophyll *a* (Chl *a*) and primary productivity. The investigations were conducted on board the R/V *Beidou* (summer, autumn and winter cruises) and *Science No. 1* (spring cruise) in the region of 32°20′–36°40′N and west of 124°00′E, as previously described by Wei et al. (2010a) and Fu et al. (2009a). Because this study aims to discern the physical-biogeochemical processes and ecological responses in individual areas in the SYS, the selected stations and data relevant to specific subregions are derived from these cruises and shown below.

Moreover, observed salinity data in the Subei Shoal and its adjacent areas, which were collected on board the R/V *Science No. 2* in August 2011, were compiled in this study; the stations are shown in Fig. 12. In addition, the data (temperature, salinity, nutrients and Chl *a*) along a cross-section of the central SYS, which were collected on board the R/V *Xiangyanghong No. 8* during September 9–10, 2010, were integrated into the study as well. The stations are shown in Fig. 17a.

The hydrological parameters (temperature, salinity, density, and turbidity) of seawater were measured using a Sea-Bird conductivity–temperature–depth (CTD) profiler (Sea-Bird Electronics, Bellevue, WA, USA). Nutrient samples were analyzed by spectrophotometry after filtration through cellulose acetate-fiber filters, which were pretreated by soaking in 1% (v/v) HCl for 24 h and then washed with Mill-Q water to a neutral pH. As to the measurement of SPM, the filter membranes were burned at ~50°C for ~5 h and weighed in advance, and the SPM sample on the filter membrane was also dried and weighed; subsequently, SPM content was determined by the weight difference. Chl *a* samples were filtered through GF/F filters and then frozen quickly at –20°C in the dark until laboratory analysis; and Chl *a* was extracted in 90% (v/v) acetone and measured using a TD-700 fluorometer (Turner Designs, Sunnyvale, CA, USA). Primary productivity was measured using the isotopic (^{14}C) tracer method established by Nielsen (1952). Note that the analytical methods of relevant hydrological and biogeochemical parameters obtained from the cruises during 2006–2007 can also be found elsewhere (Wei et al., 2010a; Fu et al., 2009a, b), but the data were used from different perspectives previously.

3 Results and discussion

3.1 *Hydrological settings based on satellite-derived data*

Figure 2 shows the distributions of SST in the SYS. In winter (Fig. 2a), a tongue-shaped high-temperature water mass extended from the southeastern SYS toward the northwest, indicating the intrusion of the YSWC (Lie et al., 2009, 2019). The low-temperature waters bypassing Shidao moved southwestward into the SYS. This cold water is primarily the result of the southward-flowing YSCC (Guo, 1993). The waters along the Subei coastline were characterized by relatively low temperatures and extended pinnately toward the southeast, suggesting the existence of the Subei Coastal Water (SCW) (Zhang, 2014; Wu et al., 2018), which mainly originates from the multiple Subei local rivers and the remnant CDW (Wu et al., 2014; Zhu and Wu, 2018). Furthermore, during the northward intrusion of the YSWC from the southeast, the route of this current was varied, and the YSWC could generally be divided into two branches near the 35°N section. One branch extended toward the Haizhou Bay and the Qingdao coastline to the south of the Shandong Peninsula, while the other branch turned to the north/northeast and headed to the NYS. This finding reveals a westward shift of the YSWC toward the south of the Shandong Peninsula (Huang et al., 2005; Zhao et al., 2011; Wang et al., 2012; Xiong et al., 2019; Wei et al., 2019). In addition, an "S"-shaped front was distinctly formed by the high-temperature YSWC and the low-temperature coastal waters.

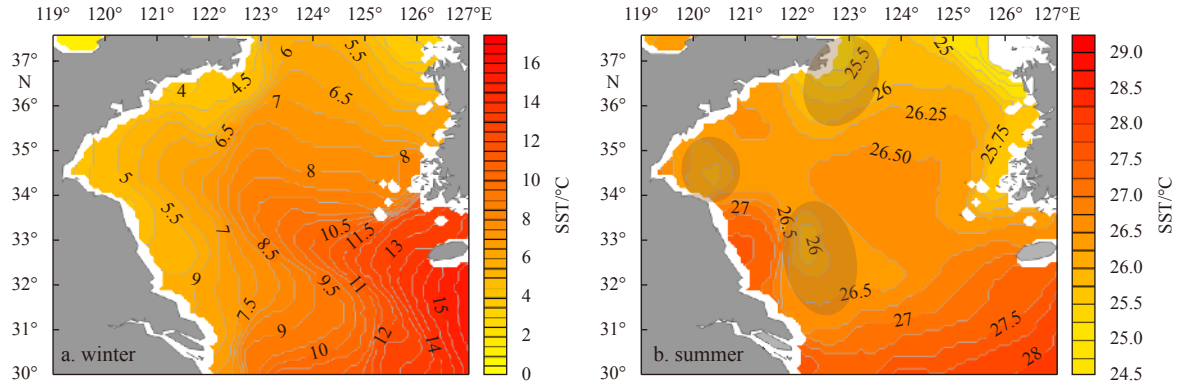

Fig. 2. Distributions of satellite-derived SST (°C) in the SYS during winter (a) and summer (b). The three shaped areas in b indicate the general locations of the upwelled cold water in the western SYS in summer.

In summer, the hydrological conditions of the SYS varied significantly. The most important hydrological characteristic was the existence of three isolated low-temperature areas (Fig. 2b), which were located in the Chengshanjiao-Shidao coast to the east of the Shandong Peninsula, in the offshore area off the Subei Shoal, and in the Haizhou Bay, respectively. These three low-temperature areas suggest the upwelling of bottom cold water, as revealed by previous studies (Zhao, 1987; Lü et al., 2010). In contrast, temperatures in the Subei Shoal and the central SYS were relatively high. Additionally, the high-temperature waters in the Subei Shoal expanded to the northeast, which was different from the orientation of the low-temperature waters in this area during winter, implying that there is a difference in the transport and expansion of the SCW during winter and summer in the Subei Shoal. Notably, although the YSCC, YSWC and SCW were recognized mainly based on the distribution patterns of satellite-derived SST, their arrangements are generally consistent with the current measurements (Yuan and Hsueh, 2010; Qiao et al., 2011; Lie and Cho, 2016; Yuan et al., 2017) through simulations, and/or moored current meter observations and/or drifter tracking.

3.2 *Spatiotemporal variations and heterogeneity of physical-biogeochemical processes in the SYS*

3.2.1 *Transport of biogenic substances and potential ecological effects off Shidao*

Figure 3 shows the distributions of temperature and nutrients in the area off Shidao. A low-temperature water mass intruding toward the southwest was present along the Shidao coast, and high-temperature waters occurred on its eastern side (Fig. 3b). As indicated by the temperature distributions along the sections off Shidao (Figs 3c, f), there was a low-temperature belt in the western coastal region, while seawater temperatures were relatively high in the eastern deep area. Furthermore, a high-nutrient area existed from the bottom to the surface in the western coastal region of the sections (Figs 3d, e, g, h), and its location generally corresponded to that of the low-temperature belt. Based on the analyses in Section 3.1, the low-temperature region off Shidao was formed by the intrusion of the YSCC bypassing the Shandong Peninsula, whereas the high-temperature waters in the offshore deep area were primarily affected by the northward-moving YSWC. Due to the relatively high nutrient concentrations in the coastal waters, the southward transport of nutrients may occur along the Shidao coastline, forming a transport belt of biogenic substances along with the YSCC. In fact, this pathway can even influence the sediment transport and sediment budget off the Shandong Peninsula (Wu et al., 2019), leading to high SPM content off Shidao in cold seasons (Wei et al., 2013c).

The YSCC-induced transport belt of biogenic substances off Shidao also existed in spring. The southward-flowing cold water along the Shidao coast (Fig. 4b), the low-temperature zone with low salinity (Figs 4c, d) and the high-nutrient region (Figs 4f, g) in the western coastal area of the 36.3°N section were clearly evident. Furthermore, as indicated by the vertical distributions of hy-

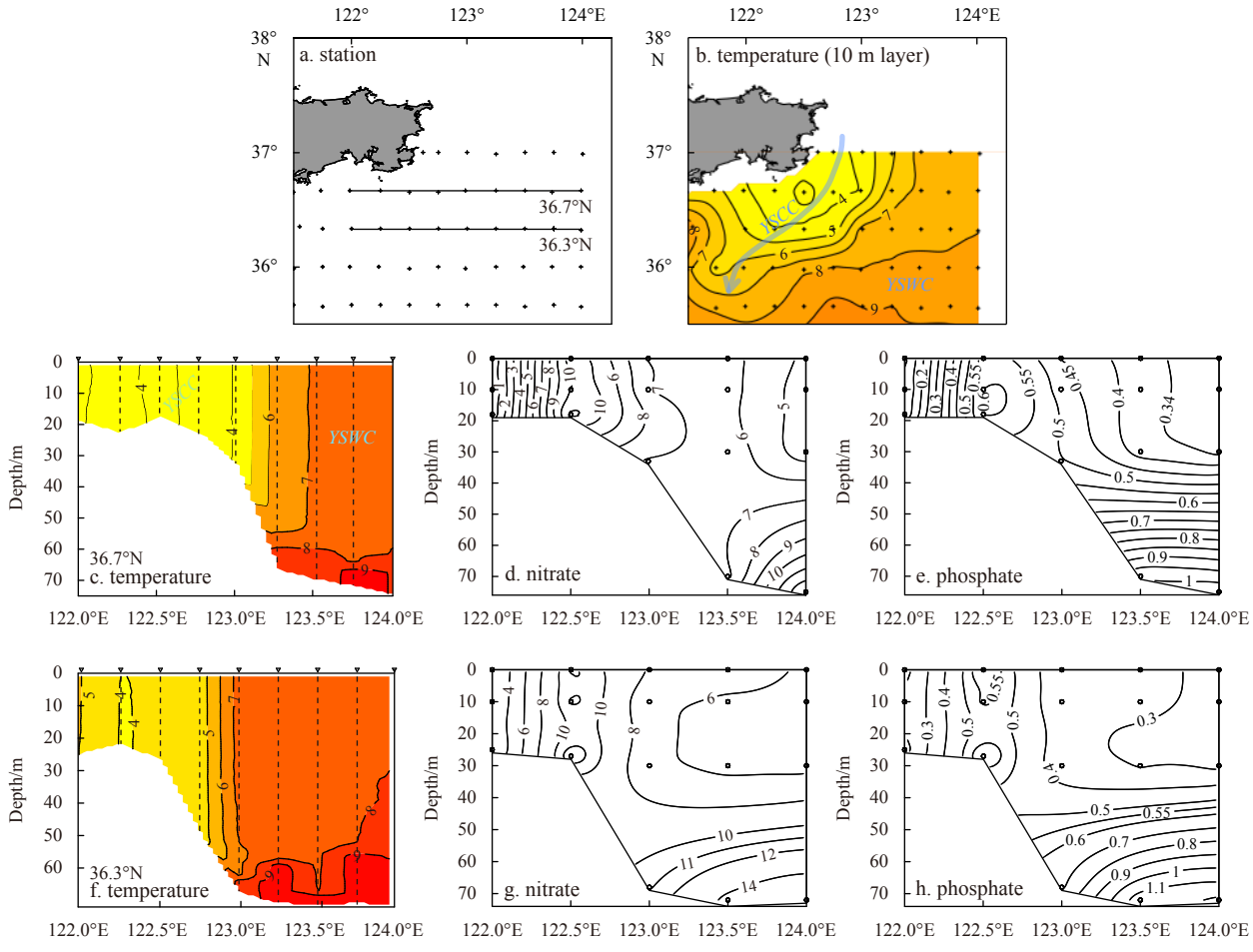

Fig. 3. Distributions of temperature (°C) and nutrients (μmol/dm³) off Shidao in winter.

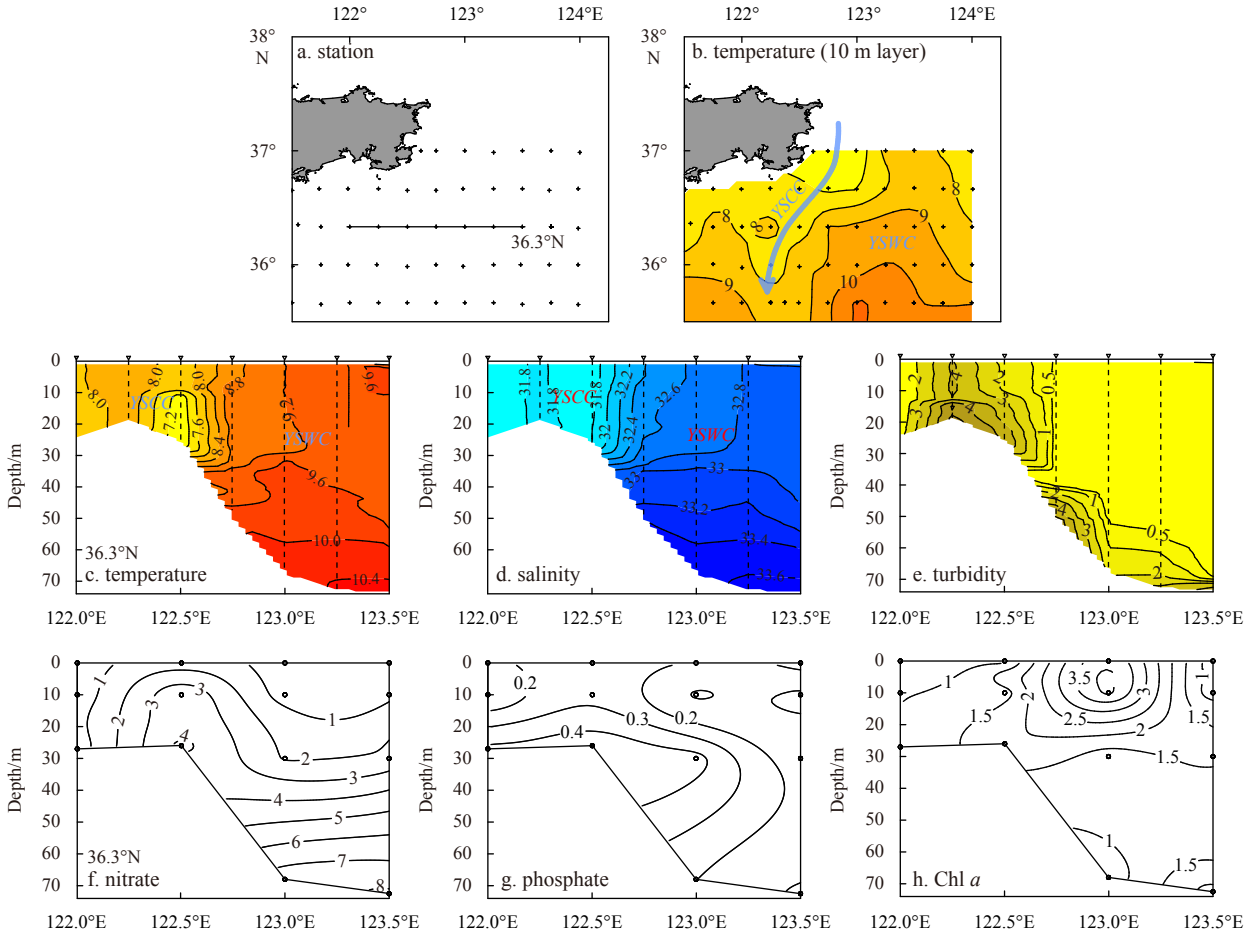

Fig. 4. Distributions of temperature (°C), salinity, turbidity, nutrients (μmol/dm³), and Chl *a* (μg/dm³) off Shidao in spring.

dro-chemical parameters along the typical section of 36.3°N, the turbidity in the transport belt was relatively high (Fig. 4e), but the Chl *a* concentration was low (Fig. 4h). This low level of Chl *a* in the YSCC-influenced region might be primarily due to light limitation; additionally, the strong mixing and low temperatures in this shallow area were not conducive to maintaining phytoplankton growth. However, in the YSWC-affected warm area, which was to the east of the YSCC-induced transport belt, the water column stability increased, and the turbidity was greatly reduced (Figs 4c–e). Therefore, the YSWC-dominated area was characterized by high Chl *a* concentration in upper layers (Fig. 4h), implying the occurrence of phytoplankton blooms in spring (Fu et al., 2009a; Jin et al., 2013).

In summer, a closed low-temperature region (<16°C) in the 10-m layer (Fig. 5b) was present off Shidao. In addition, as indicated by the vertical distribution of temperatures along the typical section of 36.3°N, the Shidao coast was stratified, and the waters underneath the thermocline were occupied by the low-temperature YSCWM (Fig. 5c). Remarkably, the shoreward uplift of cold bottom water from the YSCWM was also observed along the 36.3°N section (Fig. 5c). These phenomena suggest the existence of upwelling off Shidao. As a result, the vertical transport of biogenic nutrients occurred in this upwelling area (Fig. 5d).

Notably, with the consumption of nutrients by the spring bloom, the growth of phytoplankton can be gradually limited in the central SYS (Zhou et al., 2013). Moreover, due to the increasing temperature and decay of convective mixing, the stability of the water column in the nearshore region is strengthened from spring to summer. In this context, the location of the high Chl *a* area may transfer from offshore to nearshore. As shown in Fig. 5e, a high Chl *a* area typically appeared near 122.5°E along the 36.3°N section, whose location was more shoreward than in spring (Fig. 4h) and coincided with the position of the nearshore transport belt in spring (Figs 4f, g). The nutrients carried along the YSCC during cold seasons may constitute an early material basis for phytoplankton growth in the nearshore area off Shidao. However, with the pre-consumption of nutrients transported by the YSCC in cold seasons, the supplementation of nutrients from summer upwelling can play a role in the continuous maintenance of primary production in the Shidao coast. Actually, this seasonal alternation between the southward YSCC-driven transport in spring and upwelling-induced vertical delivery in summer could also be observed along the section of 36.7°N (Fig. 6).

3.2.2 *Hydrological processes and biogeochemical responses in the area adjacent to the Haizhou Bay*

Figure 7 shows the distributions of surface temperature in the area adjacent to the Haizhou Bay from winter to summer. As indicated by Fig. 7b, in winter, the northwestward branch of the YSWC significantly affected the Haizhou Bay and the coastal region off Qingdao. In spring (Fig. 7c), the YSCC transported cold waters toward the south, generating a low-temperature area outside of the Haizhou Bay. In summer (Fig. 7d), an isolated cold-water patch was observed in the area adjacent to the Haizhou

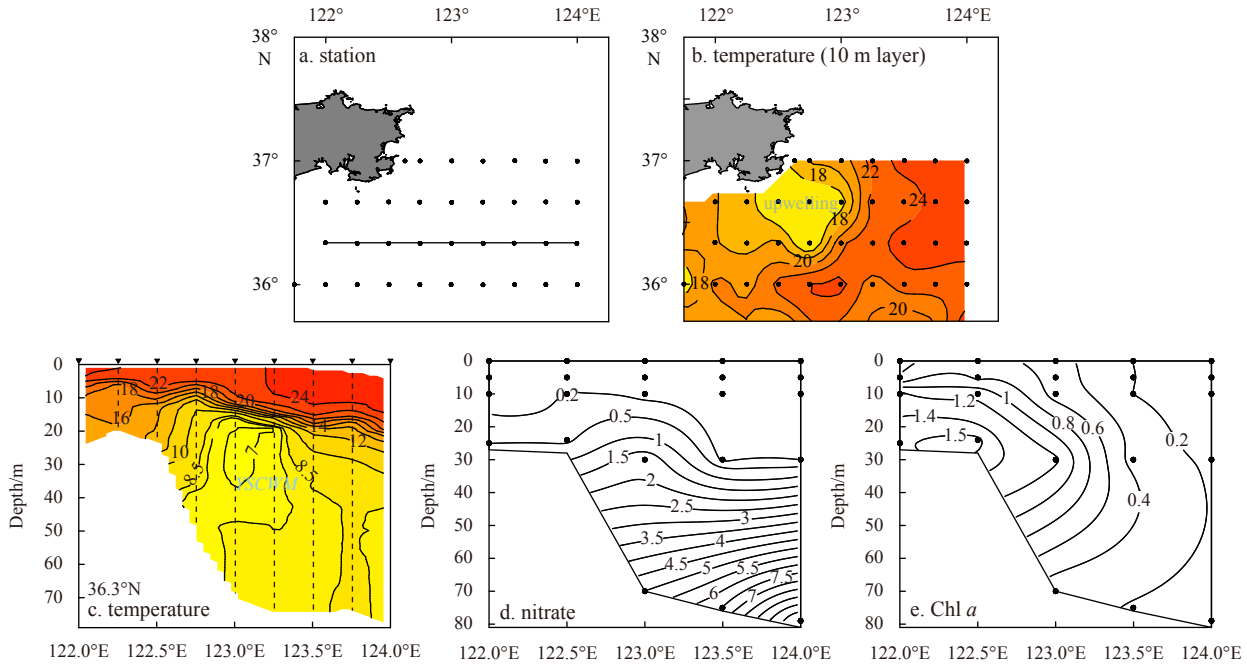

Fig. 5. Distributions of temperature (°C), nitrate (μmol/dm^3) and Chl *a* (μg/dm^3) off Shidao in summer (the patterns of other main nutrients such as phosphate are similar to those of nitrate and are therefore not shown).

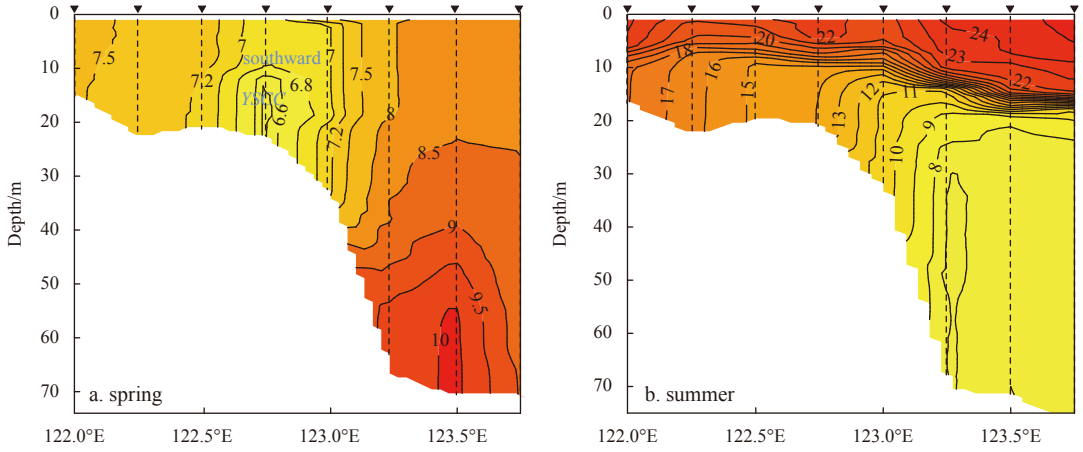

Fig. 6. Distributions of temperature (°C) along the 36.7°N section across off Shidao. The location of the section is shown in Fig. 5a.

Bay. As shown by the vertical distributions of temperature along the 35°N section, the areas beyond the Haizhou Bay could be influenced by the western front of the high-temperature YSWC in winter (Fig. 8a). In spring (Fig. 8b), the southward YSCC produced a cold-water region near 122°E, and a front was formed between the cold water and the eastern YSWC. In summer (Fig. 8c), the entire section was stratified, and the thermocline was uplifted in the western nearshore area, which led to a shoreward upwelling around the boundary of the YSCWM. A comparison of Fig. 8b and Fig. 8c indicates that the cold water transported by the YSCC in spring could form a source of the YSCWM water near 122°E along the 35°N section in summer. Furthermore, the upwelling of bottom cold waters was responsible for the surface isolated low-temperature area outside of the Haizhou Bay. These results not only confirm the role of cold waters along with the southward YSCC in the western SYS during cold seasons in the formation of the YSCWM in warm seasons, but also demonstrate that portions of these cold waters can upwell to the upper layers outside of the Haizhou Bay in summer. Consequently, the above-mentioned hydrological settings constitute the driver of biogeochemical and ecological processes in the area adjacent to the Haizhou Bay. The distributions of phosphate and Chl *a* along the 35°N section in summer (Fig. 9) verified the upwelling-induced nutrient supplement and enhanced primary production in the upper layers outside of the Haizhou Bay.

3.2.3 *Offshore/onshore transport and potential ecological effects in the Subei coast*

As indicated by Fig. 10, an area with high SPM content was observed off the Subei coast from spring to autumn, and the SPM content exhibited a nearshore-offshore decreasing trend. Moreover, Fig. 10 suggests that the transport direction of the SPM off the Subei coast was different between cold and warm seasons, moving toward southeast during cold seasons and northeast/

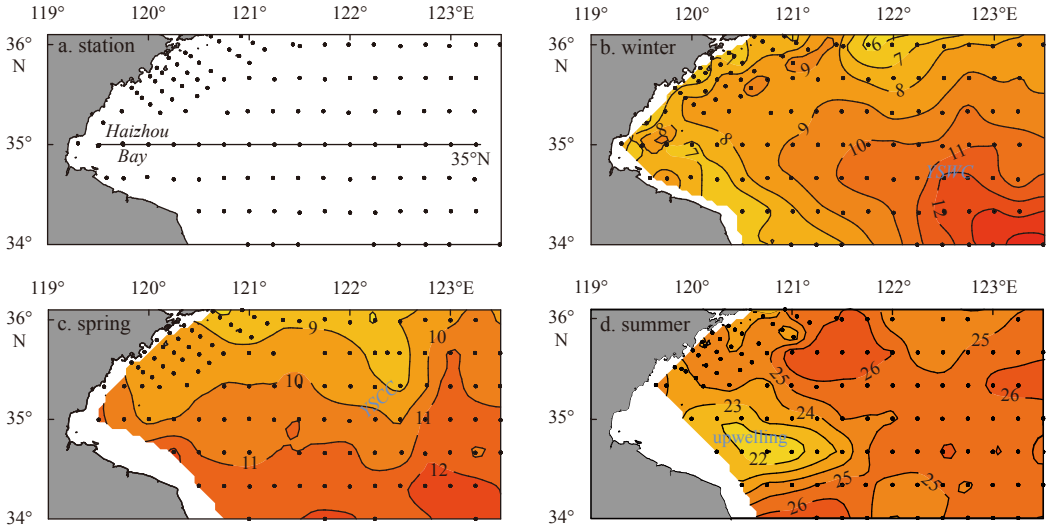

Fig. 7. Distributions of surface temperature (°C) in the area adjacent to the Haizhou Bay.

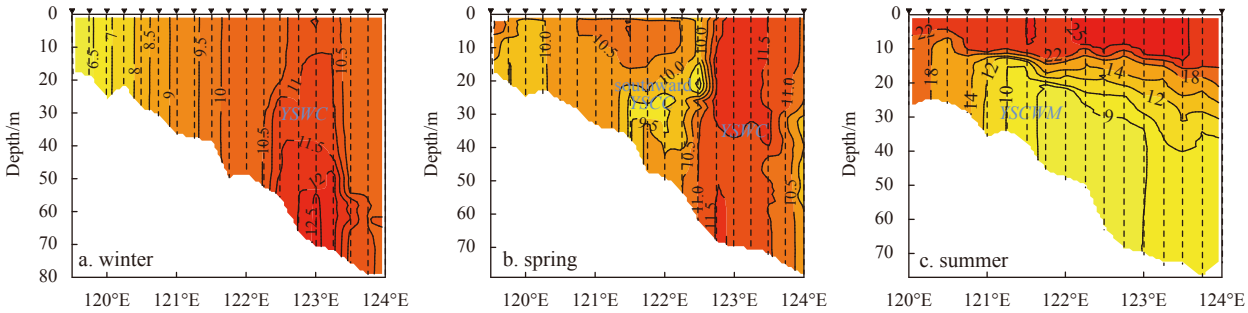

Fig. 8. Distributions of temperature (°C) along the 35°N section across the Haizhou Bay. The location of the section is shown in Fig. 7a.

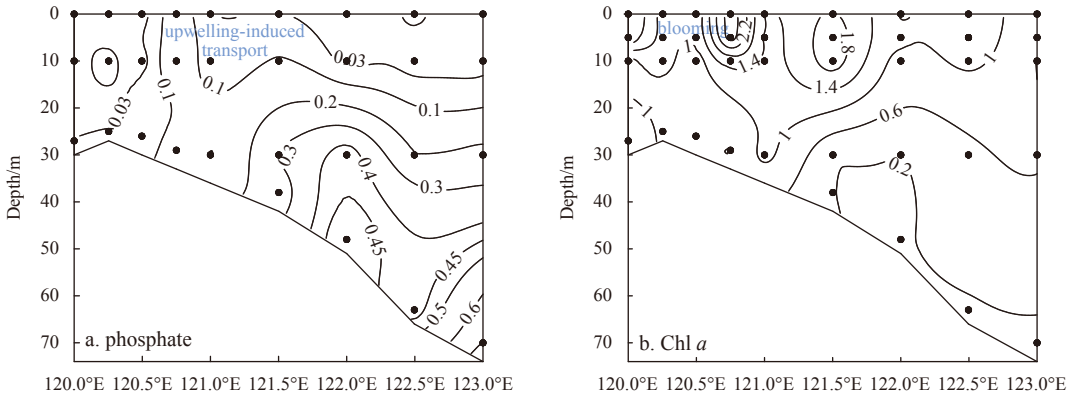

Fig. 9. Distributions of phosphate (μmol/dm³) and Chl *a* (μg/dm³) along the 35°N section in summer (the distribution patterns of other main nutrients such as nitrate are similar to those of phosphate and hence are not shown).

north during warm seasons. Additionally, during the southward transport of SPM in spring, the horizontal delivery was initially triggered around the Old Huanghe Mouth to the area near the southern Subei Shoal; because the northward-moving waters with relatively low levels of SPM created a barrier, the movement reverted to the southeast for a cross-regional transport (Fig. 10a). This process demonstrates the offshore transport in the Subei coast during cold seasons, which can be further supported by numerical simulations and remote sensing (Wang et al., 2017; Sun et al., 2018).

As revealed by Wei et al. (2018), the low-salinity and low-density SCW in the Subei Shoal expands northeastward in summer, whereas the offshore subsurface waters are upwelled near the 20- to 30-m isobaths, inducing an upwelling front beyond the coastal waters. Furthermore, we find that the saline and dense upwelling belt off the Subei Shoal in summer could be divided into three subareas: the northern part (Area I), eastern part (Area II) and southern part (Area III) (Fig. 11). Notably, the dense and saline waters in Areas I and II were mainly caused by tidal mixing around the YSCWM (Zhao, 1987; Lü et al., 2010), and the

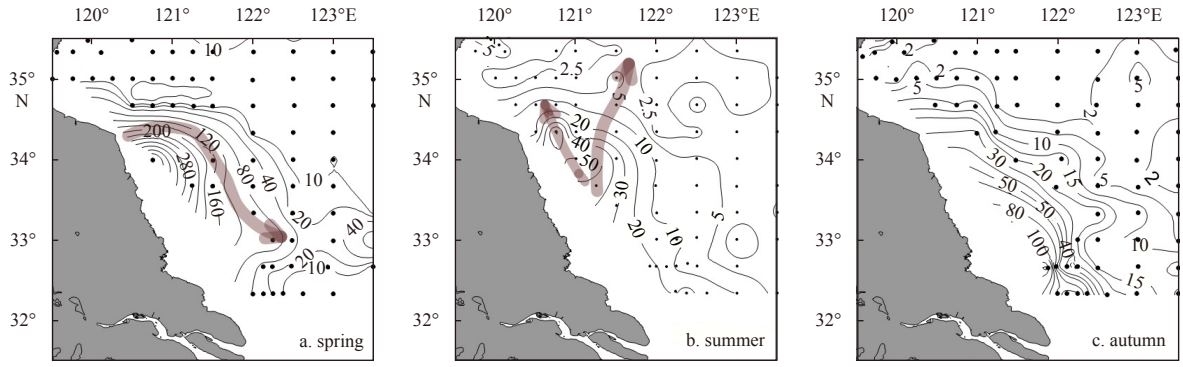

Fig. 10. Distributions of SPM (mg/dm³) in the 10-m layer of the Subei Shoal and its adjacent areas from spring to autumn. Arrows generally indicate the orientation of SPM transport.

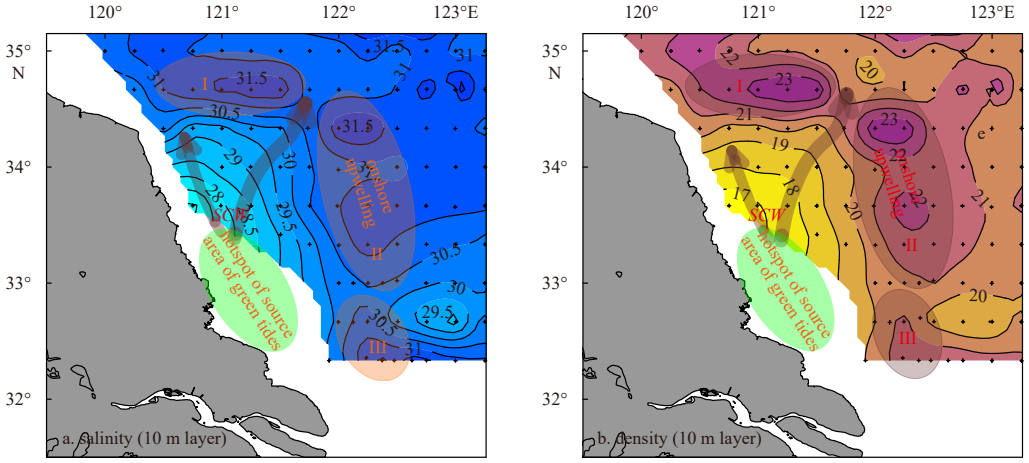

Fig. 11. Distributions of salinity and density (kg/m³) in the 10-m layer of the Subei Shoal and its adjacent areas in summer of 2006. Arrows indicate the potential expansion routes of coastal waters from the Subei coast; the shaded ellipses with red captions overlaid the maps indicate the three subareas of upwelling off the Subei Shoal; and the hotspot of the source area of green tides is sourced from Wang et al. (2015b) and Xing et al. (2019).

dense and saline waters in area III were associated with the upwelling of the TWC frontal waters (Wei et al., 2017). Additionally, during the northeastward offshore expansion of the SCW in the Subei Shoal, the outward transport primarily occurred in the region between the northern and eastern saline areas (i.e., Areas I and II) off the shoal (Fig. 11), where the topography is relatively steep (Fig. 1a). This phenomenon is further indicated by the distribution of SPM in summer (Fig. 10b). As a result, Areas I and II were partially separated. Furthermore, in summer, parts of the low-salinity and low-density water in the Subei Shoal moved northward along the coast (Fig. 11). Thus, Fig. 10 suggests two potential expansion/transport routes of coastal waters. The surface salinity distribution in the Subei coast and its adjacent areas in August 2011 also exhibits a northeastward expansion of the low-salinity SCW (Fig. 12a), whereas the low-salinity waters in bottom layer were primarily restricted to the shoal area (Fig. 12b). These findings considerably refine the understanding of the hydrodynamics and the interactions between the SCW and offshore upwelling in the Subei Shoal and its adjacent areas.

Offshore/onshore transport in the Subei coast has distinct impacts on regional biogeochemical and ecological processes. The distribution of satellite-derived SST in winter (Fig. 2a) indicates that the southeastward offshore transport of the SCW and the shoreward extension of the high-temperature YSWC represented a pathway of cross-regional material exchange during cold seasons. As a result, an area with high SPM and nutrients is induced in the northern ECS in winter and spring, as previously revealed by Wei et al. (2013b, 2016b). Notably, in recent years, green tides caused by *Ulva prolifera* have frequently occurred during warm seasons in the Subei Shoal (Liu et al., 2013; Zhou et al., 2015; Wang et al., 2015b). Evidentially, the northeastward expansion of coastal waters in the shoal could form an important physical driver for the offshore transport of *Ulva prolifera* from the coast (Fig. 11). This is further supported by the numerical experiment results of Lee et al. (2011). Additionally, induced by the northeastward movement of low-salinity waters from the Subei Shoal, some nutrients may be transported into the offshore region from the coastal area, as indicated by the nutrient distributions in the Subei Shoal and its adjacent areas during summer (Pan et al., 2018). Consequently, it is conceivable that the nutrients transported by the upwelling system off the Subei Shoal and these carried by the low-salinity waters from the coast can jointly affect the proliferation and biomass of drifting *Ulva prolifera* along the way.

3.2.4 *Seasonal stratification and frontal system of the YSCWM area and their effects on biogeochemical processes*

As shown in Fig. 13, the temperature distributions along the

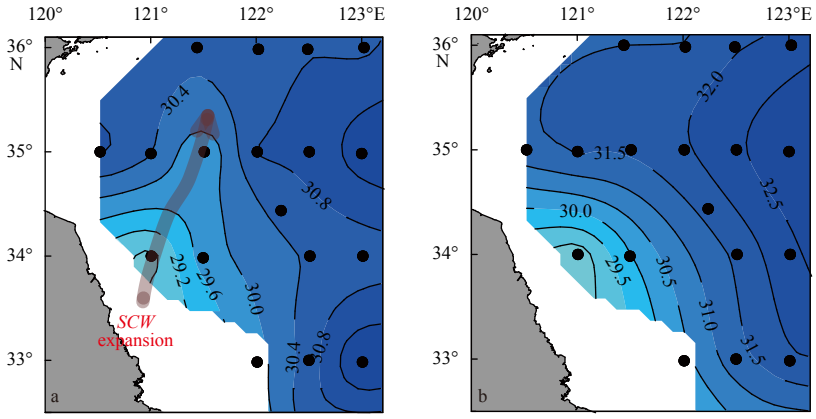

Fig. 12. Salinity distributions in the surface (a) and bottom (b) layers of the Subei Shoal and its adjacent areas in August 2011.

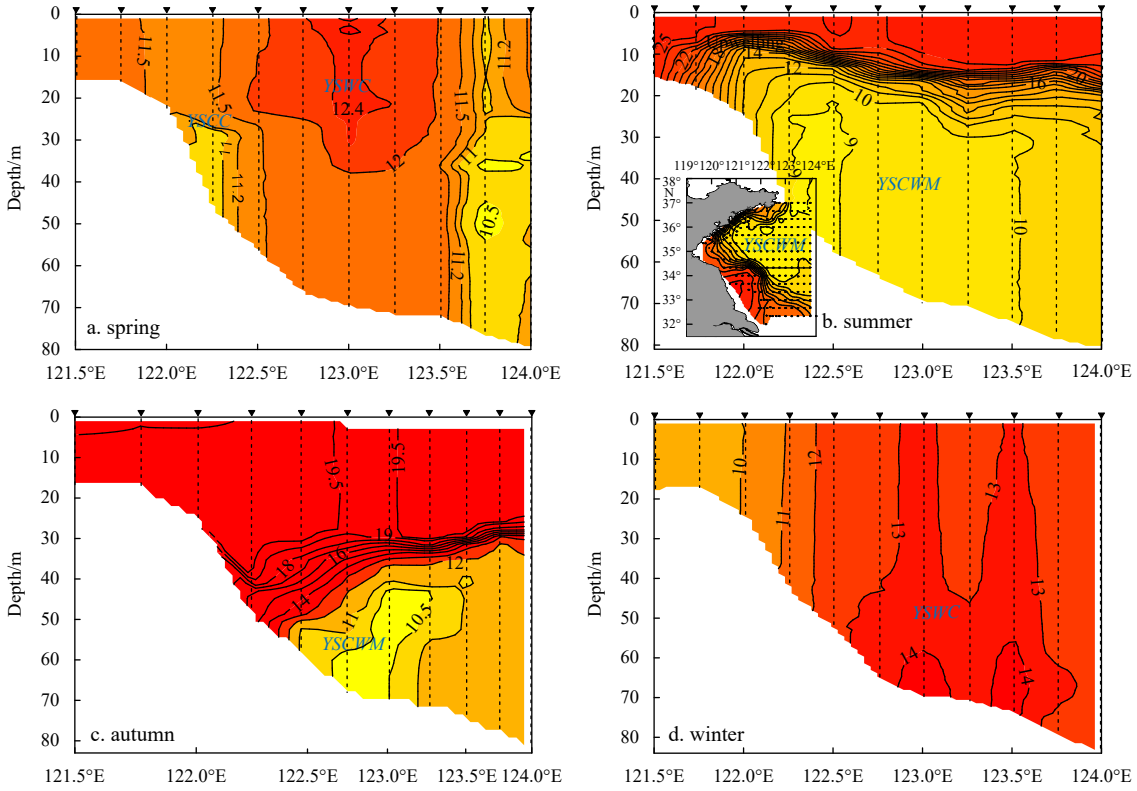

Fig. 13. Seasonal distributions of temperature (°C) along the 34.3°N section across the YSCWM area. The inset in b shows the location of the 34.3°N section and the summer bottom temperature distribution in the SYS.

34.3°N section highlighted the seasonal stratification and unique frontal system of the YSCWM in the SYS. In spring, due to increasing temperatures in the upper layers, the stratification signal began to appear in the central area of the section (Fig. 13a). In summer, the entire section was strongly stratified, and the area underneath the thermocline was occupied by the YSCWM (Fig. 13b). In autumn, accompanied by increases in wind stress and decreases in surface temperature, the mixing of the upper-layer waters was promoted, and the depth of the thermocline deepened (Fig. 13c). In addition, the YSCWM retreated to deep waters, and the stratification strength was weakened. In winter, due to strong vertical mixing, the stratification structure decayed (Fig. 13d). As indicated by Fig. 13, the frontal system of the YSCWM in warm seasons was closely associated with stratification. Typically, the frontal zone was located near the edge of the stratified area (i.e., the boundary of the YSCWM), and the expansion and reduction of this area corresponded to the movement of the front. Importantly, the upwelling of cold water from the YSCWM was clearly observed in the frontal zone in summer (Fig. 13b). Notably, caused by the southward movement of the YSCC in the western part of the SYS, a low-temperature area (< 11.5°C) was present near 122.25°E (i.e., off the Subei Shoal) in spring (Fig. 13a). Evidentially, the cold water transported by the YSCC in spring could form a source of the YSCWM water near 122.25°E over the 34.3°N section in summer (Fig. 12b), similar to the case of the 35°N section (Figs 8b, c).

As shown in Fig. 14, nutrient concentrations in the upper-layer waters (⩽30 m) of the central SYS (station depth>40 m) exhib-

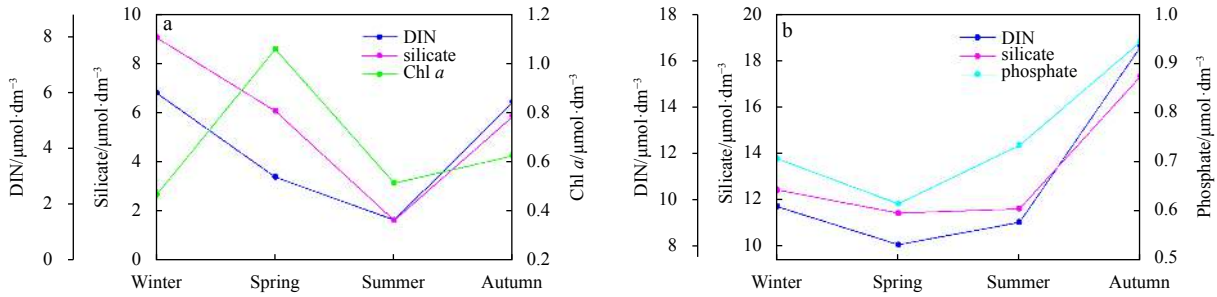

Fig. 14. Seasonal variations in environmental parameters in the central SYS. a. Upper layer waters and b. bottom layer waters.

ited a decreasing trend from winter to summer, whereas the nutrients in the bottom layer displayed an increasing trend from spring to autumn; and Chl *a* concentraions in the upper layers reached a maximum value in spring. These results imply the regulation functions of stratification and biogeochemical processes on the spatial distribution of nutrients in the central SYS. Beginning in spring, the phytoplankton reproduction gradually reduces the nutrient concentrations in the upper layers, and the nutrients in the stratified upper waters are decreased to a minimum value in summer. From spring to autumn, the nutrients regenerated from the decomposition of organic matters can be accumulated in the bottom layer. These biogeochemical processes can lead to decreases in dissolved oxygen (DO) and pH and increases in apparent oxygen utilization (AOU) in the bottom waters of the central SYS from spring to autumn (Wei, 2016), thus yielding seasonal acidification, as also indicated by Zhai (2018).

Notably, due to the barrier effects of stratification on the vertical diffusion of nutrients from the subsurface, phytoplankton blooms occurring in the central SYS in spring gradually disappear in summer (Fu et al., 2009a; Zhou et al., 2013). As indicated by the statistical correlations between the surface temperature, surface Chl *a*, primary productivity and the water depth in the western SYS in summer 2006 (Fig. 15), the high-value areas (approximately 15-m to 35-m isobaths) of surface Chl *a* and primary productivity were generally consistent with the surface low-temperature upwelling zone. Indeed, in the surface cold-water patches formed by the upwelling around the YSCWM in summer, Chl *a* concentration was positively correlated with nutrient, as previously revealed by Wei et al. (2016b). These results reflect the role of the upwelling system in maintaining primary production at a depth range of 15–35 m in the western SYS in summer. Subsequently, the high Chl *a* areas may be transferred from the central SYS in spring to the YSCWM boundary in summer. The distributions of Chl *a* along the typical sections in spring and summer further confirmed this phenomenon (Fig. 16). In addition, as indicated by the distributions of temperature, salinity, nitrate and Chl *a* along the cross-section of the central SYS in September 2010 (Fig. 17), a westward uplift of low-temperature and saline waters from the YSCWM area occurred, resulting in the vertical transport of nutrients from the YSCWM and enhanced Chl *a* concentration in the upper-layer waters. Notably, as the YSCWM retreated seaward to deeper areas in September than in July (Fig. 8c), the upwelling position, which was related to the YSCWM boundary, also moved seaward in September (Figs 17b, c).

3.3 *Intrinsic connectivity of the physical-biogeochemical processes in different subregions and associated mechanisms in the SYS*

Although the physical-biogeochemical processes in different areas of the SYS have been distinguished individually, their intrinsic connections and mechanisms are further demonstrated. With regard to hydrological processes, the cold waters that moved southward bypassing the Shandong Peninsula, and the low-temperature waters that extended to the southeast in the Subei Shoal interacted with the northward YSWC waters in the central SYS during cold seasons. Subsequently, a significant "S"-shaped front could be formed in the SYS in winter (Fig. 2a). In addition, the southward cold waters off Shidao caused the YSWC to form a dual tongue-shaped structure (Fig. 2a). Notably, in spring, the southward cold waters bypassing the Shandong Peninsula extended beyond the Haizhou Bay (Fig. 8b) and flowed to the east of the Subei Shoal (Fig. 13a), partially comprising a source of cold waters in the western part of the YSCWM in summer. During warm seasons, the upwelling around the YSCWM boundary may act as a transitional zone connecting the stratified area and the

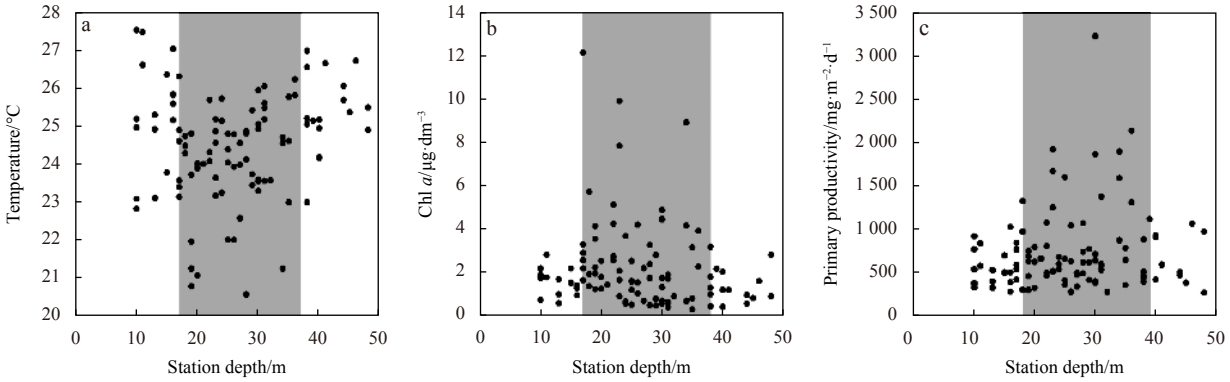

Fig. 15. Statistical correlations between the surface temperature (a), surface Chl *a* (b), primary productivity (c) and the water depth in the western area (station depth<50 m) of the SYS in summer 2006.

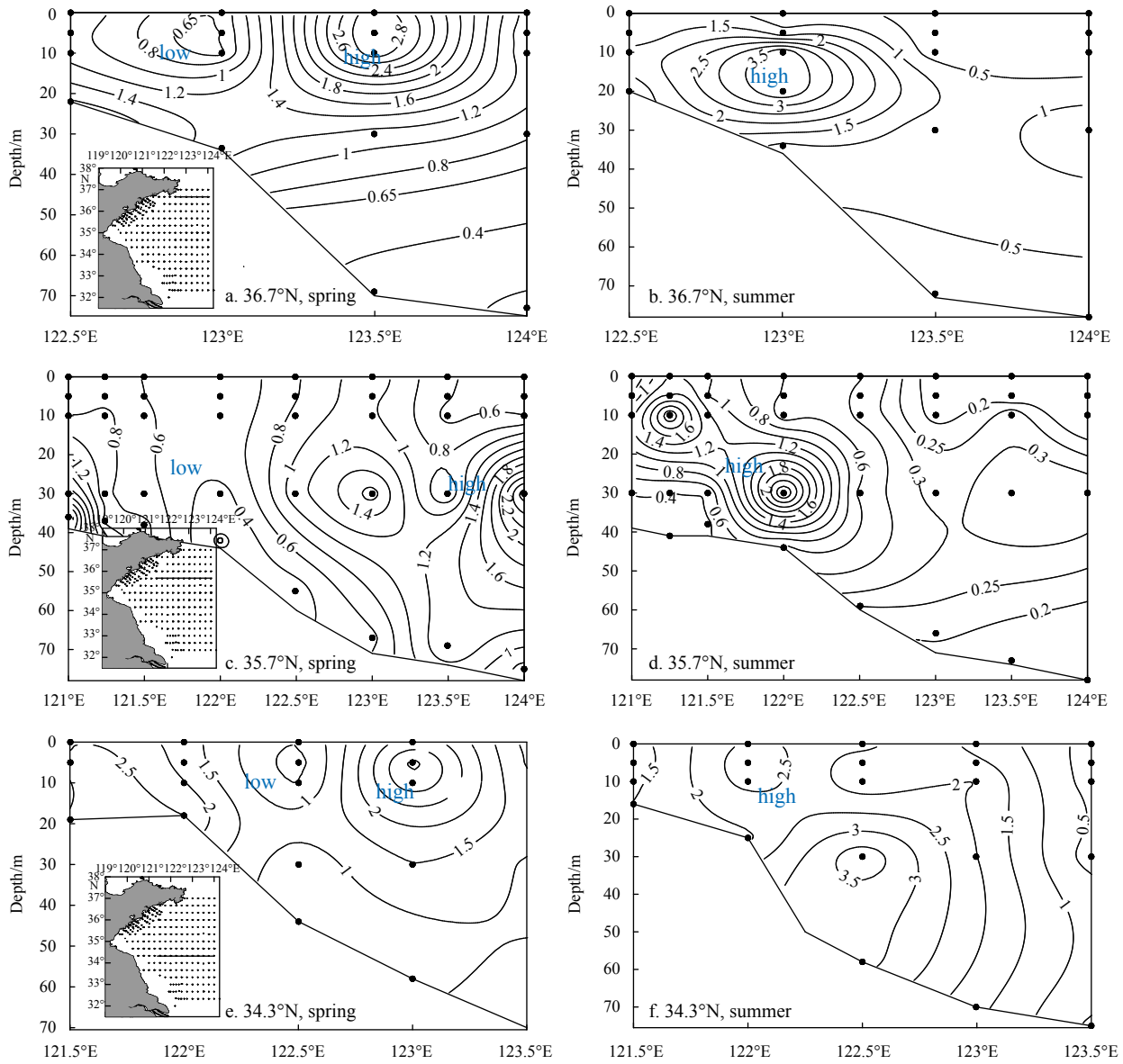

Fig. 16. Distributions of Chl *a* (μg/dm^3) along the 36.7°N, 35.7°N and 34.3°N sections in spring and summer. Insets in a, c and e display the locations of the relevant sections.

coastal region. Therefore, the entire SYS can be divided into a nearshore vertically mixed zone, an upwelling area near the front and an offshore stratified zone in summer. Due to the inhomogeneous upwelling intensity around the YSCWM boundary in summer, the Shidao coast, the area beyond the Haizhou Bay and the area off the Subei Shoal represented three typical areas, where a closed low-temperature zone were formed in the upper layers (Fig. 2b). Moreover, according to the seasonal evolution of the YSCWM, the front around the YSCWM boundary was closest to the shoreline in summer; thus, the impact of upwelling on the nearshore regions might be the strongest during summer, as indicated in Fig. 13b. When autumn arrived, the YSCWM retreated back to the deep area and the front moved eastward; correspondingly, the nearshore mixed area extended offshore (Fig. 13c).

Regarding the biogeochemical and ecological processes, the nutrients transported with the YSCC off Shidao and in the area adjacent to the Haizhou Bay in cold seasons may comprise the early material basis for phytoplankton growth. When this transport decays in summer, the upwelling in these two areas can supply nutrients to the euphotic layer. Therefore, a seasonal alternation is achieved between the YSCC-induced delivery in cold seasons and the upwelling-induced transport in warm seasons off Shidao and in the area adjacent to the Haizhou Bay. In the YSCWM-dominated central SYS during stratified warm seasons, due to the continuous uptake of nutrients by phytoplankton, the level of nutrients is relatively low above the thermocline, whereas the nutrients are regenerated and accumulated in the bottom layer. Therefore, in warm seasons, the YSCWM may act as an important reservoir/pool of nutrients (Fig. 17d). More importantly, during warm seasons, the upwelling system around the YSCWM boundary can extract nutrients from the YSCWM and connect the biogeochemical processes between the internal cold-water mass area and the frontal region, resulting in the overall consistency among the high Chl *a* area, high primary productivity region and low-temperature upwelling zone in the SYS (Fig. 15). Accordingly, the high Chl *a* zones in surface waters are predom-

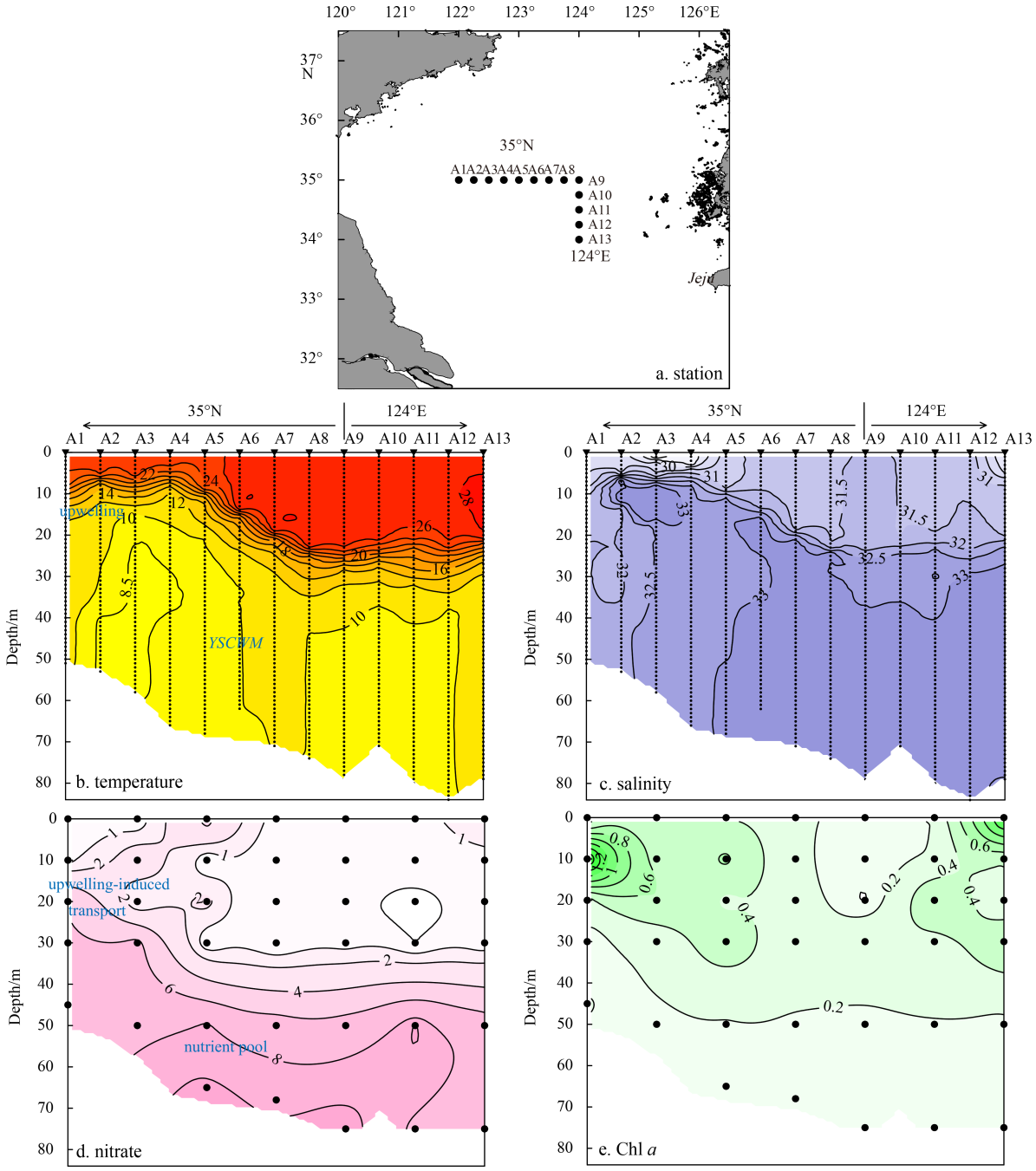

Fig. 17. Distributions of temperature (°C), salinity, nitrate (μmol/dm³) and Chl *a* (μg/dm³) along the cross-section of the central SYS in September 2010.

inantly observed beyond the Shidao coastline, Haizhou Bay and the Subei Shoal in summer (Fu et al., 2009a), where the upwelling is noticeable. Consequently, the spatiotemporal differences in the physical-biogeochemical-ecological processes are formed from the coast to offshore areas in the SYS. This may partially lead to the spatial and seasonal variability of Chl *a* in the YS (Liu and Wang, 2013; Jiang et al., 2019).

Based on the aforementioned analyses, a conceptual view illustrating the physical-biogeochemical processes and their correlations in the SYS is provided in Fig. 18. In general, the SYS contains several typical subregions, such as the Shidao coast, Haizhou Bay, Subei Shoal, YSCWM area and its frontal zone. Although each subregion has its own unique physical-biogeochemical processes, close connections also exist among them. During the cold seasons, the interactions of the southward cold waters in the western area and the northward warm waters in the central region lead to the formation of the "S"-shaped front in the SYS, partially regulating the material transport and exchange. In addition, in spring, a cold-water belt bypassing the Shandong Peninsula connects the Shidao coast, the region beyond the Haizhou Bay and the area off the Subei Shoal. During warm seasons, the upwelling system around the YSCWM boundary is the link between the stratified central area and the well-mixed nearshore zone, and three typical physical-biogeochemical-ecological

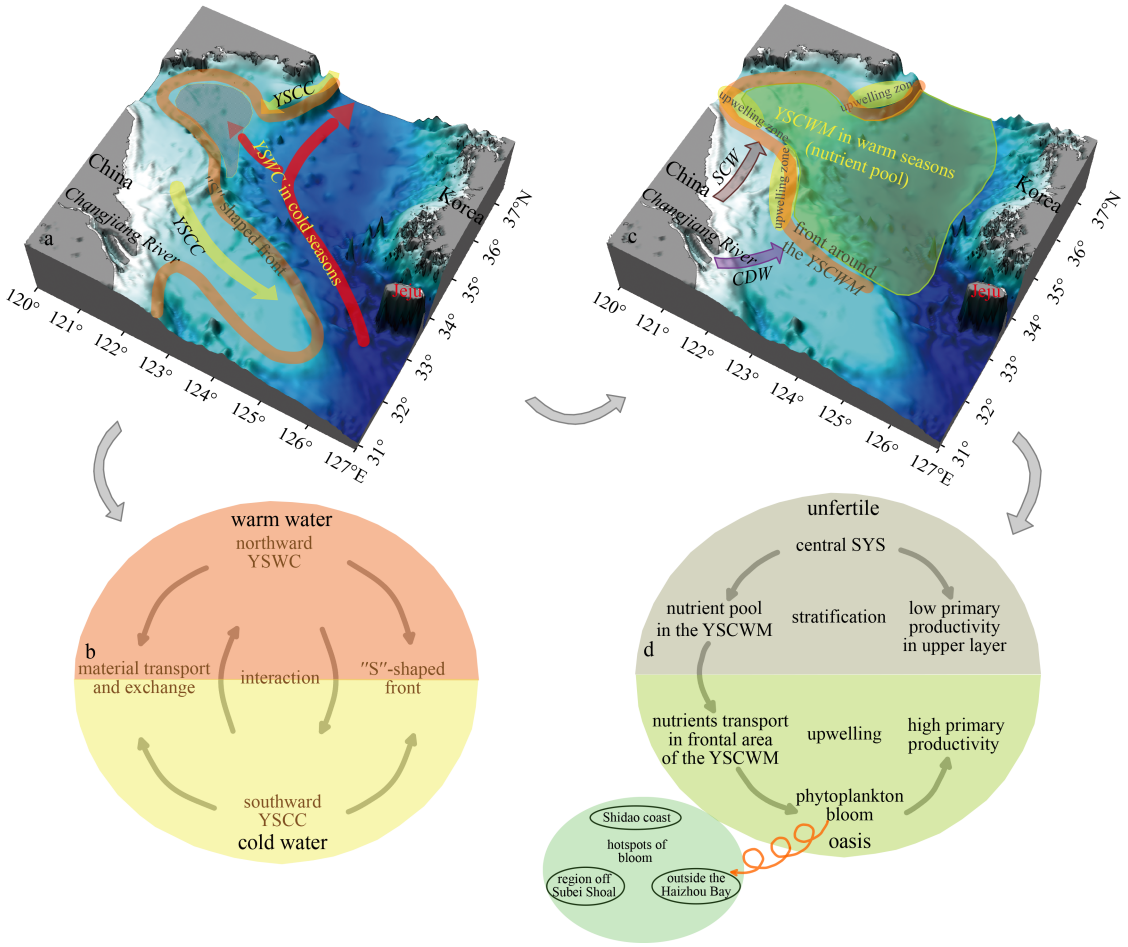

Fig. 18. Conceptual overview of the variability of physical-biogeochemical processes and correlations in the SYS during cold seasons (a, b) and warm seasons (c, d). The gray pear-shaped zone in panel a indicates the general range of remnant YSCC-transported cold waters, which comprises a source of cold waters in the western part of the YSCWM in summer.

coupling regions are generated, including the Shidao coast, the area adjacent to the Haizhou Bay and the area off the Subei Shoal. The linkage of these processes and their synergies drive and maintain the relevant ecological processes in the SYS.

4 Concluding remarks

The SYS is a complex system that comprises several typical subregions. In this study, based on a combination of remote sensing data and integrated historical observations, the spatiotemporal variability and heterogeneity of the physical-biogeochemical processes in the SYS was investigated, and the intrinsic correlations and associated mechanisms of these processes were systematically examined.

(1) The seasonal alternation between southward transport by the YSCC during cold seasons and vertical delivery by upwelling during warm seasons is the main physical control influencing the biogeochemical processes and primary production off Shidao and the area beyond the Haizhou Bay. During cold seasons, cross-regional material transport in the Subei coast first occurs from the Old Huanghe Mouth to the southern Subei coast, after which material is transported to the southeast. The northeastward expansion of coastal waters in the Subei Shoal may be an important physical driver of the offshore transport of *Ulva prolifera* in summer.

(2) Stratification significantly regulates biogeochemical processes in the YSCWM area during stratified seasons. Nutrients accumulate in bottom-layer waters from spring to autumn, making the YSCWM area an important nutrient pool. The upwelling system in the YSCWM's boundary frontal zone in summer leads to consistency among the high Chl *a* area, high primary productivity region and low-temperature upwelling zone in the SYS.

(3) Although each typical region has its own unique physical-biogeochemical processes, there are also close connections between different units. During cold seasons, the interactions of the southward YSCC in the western nearshore region and the northward YSWC in the central region lead to the formation of an "S"-shaped front in the SYS. In warm seasons, the upwelling system around the YSCWM boundary links the central stratified area and the vertical well-mixed nearshore region. The upwelling can extract nutrients from the YSCWM; thus, the biogeochemical-ecological processes inside the cold-water mass and in the frontal zone are well connected via upwelling, and three physical-biogeochemical-ecological coupling regions are generated, namely, the Shidao coast, the area adjacent to the Haizhou Bay and the area off the Subei Shoal.

This study reveals the spatiotemporal heterogeneity of hydro-biogeochemical processes and their potential correlations in the SYS, refining and deepening our understanding of regional oceanography from a comprehensive and systematic perspective. The results imply that the uniqueness of individual regions

and linkages among typical regions in the SYS should be fully considered in future studies in order to provide a detailed recognition of the biogeochemical cycles and establish a regional model to perform elaborate ecological simulations in this Large Marine Ecosystem.

Acknowledgements

We thank the anonymous reviewers for their assistance with this paper.

References

Bai Hong, Hu Dunxin, Chen Yongli, et al. 2004. Statistic characteristics of thermal structure in the southern Yellow Sea in summer. Chinese Journal of Oceanology and Limnology, 22(3): 237–243, doi: 10.1007/BF02842554

Bian Changwei, Jiang Wensheng, Greatbatch R J. 2013. An exploratory model study of sediment transport sources and deposits in the Bohai Sea, Yellow Sea, and East China Sea. Journal of Geophysical Research, 118(11): 5908–5923

Chen C T A. 2009. Chemical and physical fronts in the Bohai, Yellow and East China Seas. Journal of Marine Systems, 78(3): 394–410, doi: 10.1016/j.jmarsys.2008.11.016

Fu Mingzhu, Sun Ping, Wang Zongling, et al. 2018. Structure, characteristics and possible formation mechanisms of the subsurface chlorophyll maximum in the Yellow Sea Cold Water Mass. Continental Shelf Research, 165: 93–105, doi: 10.1016/j.csr.2018.07.007

Fu Mingzhu, Wang Zongling, Li Yan, et al. 2009a. Phytoplankton biomass size structure and its regulation in the Southern Yellow Sea (China): seasonal variability. Continental Shelf Research, 29(18): 2178–2194, doi: 10.1016/j.csr.2009.08.010

Fu Mingzhu, Wang Zongling, Sun Ping, et al. 2009b. Size structure and potential export of phytoplankton primary production in the southern Huanghai (Yellow) Sea. Haiyang Xuebao (in Chinese), 31(6): 100–109

Gattuso J P, Frankignoulle M, Wollast R. 1998. Carbon and carbonate metabolism in coastal aquatic ecosystems. Annual Review of Ecology and Systematics, 29: 405–434, doi: 10.1146/annurev.ecolsys.29.1.405

Guo Binghuo. 1993. Major features of the physical oceanography in the Yellow Sea. Journal of Oceanography of Huanghai & Bohai Seas (in Chinese), 11(3): 7–18

Guo Binghuo, Hu Xiaomin, Xiong Xuejun, et al. 2003. Study on interaction between the coastal water, shelf water and Kuroshio water in the Huanghai Sea and East China Sea. Acta Oceanologica Sinica, 22(3): 351–367

Ho C, Wang Yuanxiang, Lei Zongyou, et al. 1959. A prelimenary study of the formation of Yellow Sea Cold Mass and its properties. Oceanologia et Limnologia Sinica (in Chinese), 2(1): 11–15

Huang Daji, Fan Xiaopeng, Xu Dongfeng, et al. 2005. Westward shift of the Yellow Sea warm salty tongue. Geophysical Research Letters, 32(24): L24613, doi: 10.1029/2005GL024749

Huang Daji, Zhang Tao, Zhou Feng. 2010. Sea-surface temperature fronts in the Yellow and East China Seas from TRMM microwave imager data. Deep Sea Research Part II: Topical Studies in Oceanography, 57(11–12): 1017–1024, doi: 10.1016/j.dsr2.2010.02.003

Isobe A. 2008. Recent advances in ocean-circulation research on the Yellow Sea and East China Sea shelves. Journal of Oceanography, 64(4): 569–584, doi: 10.1007/s10872-008-0048-7

Jiang Zhibing, Chen Jianfang, Gao Yuexin, et al. 2019. Regulation of spatial changes in phytoplankton community by water column stability and nutrients in the southern Yellow Sea. Journal of Geophysical Research, 124(8): 2610–2627

Jin Jie, Liu Sumei, Ren Jingling, et al. 2013. Nutrient dynamics and coupling with phytoplankton species composition during the spring blooms in the Yellow Sea. Deep Sea Research Part II: Topical Studies in Oceanography, 97: 16–32, doi: 10.1016/j.dsr2.2013.05.002

Khim J S, Hong S, Yoon S J, et al. 2018. A comparative review and analysis of tentative ecological quality objectives (EcoQOs) for protection of marine environments in Korea and China. Environmental Pollution, 242: 2027–2039, doi: 10.1016/j.envpol.2018.06.094

Lee J H, Pang I C, Moon I J, et al. 2011. On physical factors that controlled the massive green tide occurrence along the southern coast of the Shandong Peninsula in 2008: a numerical study using a particle-tracking experiment. Journal of Geophysical Research, 116(C12): C12036, doi: 10.1029/2011JC007512

Li Jianchao, Li Guangxue, Xu Jishang, et al. 2016. Seasonal evolution of the Yellow Sea Cold Water Mass and its interactions with ambient hydrodynamic system. Journal of Geophysical Research, 121(9): 6779–6792, doi: 10.1002/2016JC012186

Lie H J. 1986. Summertime hydrographic features in the southeastern Hwanghae. Progress in Oceanography, 17(3-4): 229–242, doi: 10.1016/0079-6611(86)90046-7

Lie H J, Cho C H. 2016. Seasonal circulation patterns of the Yellow and East China Seas derived from satellite-tracked drifter trajectories and hydrographic observations. Progress in Oceanography, 146: 121–141, doi: 10.1016/j.pocean.2016.06.004

Lie H J, Cho H C, Lee S. 2009. Tongue-shaped frontal structure and warm water intrusion in the southern Yellow Sea in winter. Journal of Geophysical Research, 114(C1): C01003, doi: 10.1029/2007JC004683

Lie H J, Oh K H, Cho C H, et al. 2019. Wintertime large temperature inversions in the Yellow Sea associated with the Cheju and Yellow Sea warm currents. Journal of Geophysical Research, 124(7): 4856–4874, doi: 10.1029/2019JC015180

Lin Xiaopei, Yang Jiayan, Guo Jingsong, et al. 2011. An asymmetric upwind flow, Yellow Sea Warm Current: 1. New observations in the western Yellow Sea. Journal of Geophysical Research, 116(C4): C04026, doi: 10.1029/2010JC006513

Liu Xin, Chiang K P, Liu Sumei, et al. 2015a. Influence of the Yellow Sea Warm Current on phytoplankton community in the central Yellow Sea. Deep Sea Research Part I: Oceanographic Research Papers, 106: 17–29, doi: 10.1016/j.dsr.2015.09.008

Liu Xin, Huang Bangqin, Huang Qiu, et al. 2015b. Seasonal phytoplankton response to physical processes in the southern Yellow Sea. Journal of Sea Research, 95: 45–55, doi: 10.1016/j.seares.2014.10.017

Liu Dongyan, Keesing J K, He Peimin, et al. 2013. The world's largest macroalgal bloom in the Yellow Sea, China: formation and implications. Estuarine, Coastal and Shelf Science, 129: 2–10, doi: 10.1016/j.ecss.2013.05.021

Liu Guangxing, Kong Wei, Yang Guipeng. 2015c. Influence of tidal front on distribution of *Paracalanus Parvus* and chlorophyll a in summer over south Yellow Sea. Oceanologia et Limnologia Sinica (in Chinese), 46(1): 58–64

Liu Dongyan, Wang Yueqi. 2013. Trends of satellite derived chlorophyll-a (1997–2011) in the Bohai and Yellow Seas, China: effects of bathymetry on seasonal and inter-annual patterns. Progress in Oceanography, 116: 154–166, doi: 10.1016/j.pocean.2013.07.003

Lü Xin'gang, Qiao Fangli, Xia Changshui, et al. 2010. Upwelling and surface cold patches in the Yellow Sea in summer: effects of tidal mixing on the vertical circulation. Continental Shelf Research, 30(6): 620–632, doi: 10.1016/j.csr.2009.09.002

Nielsen E S. 1952. The use of radio-active carbon (^{14}C) for measuring organic production in the sea. Journal ICES Journal of Marine Science, 18(2): 117–140, doi: 10.1093/icesjms/18.2.117

Pan Jun, Yu Fei, Wei Chuanjie, et al. 2018. Relationship between green tide outbreak and nitrate and hydrological environmental factors in the south Yellow Sea. Oceanologia et Limnologia Sinica (in Chinese), 49(5): 1031–1037

Qiao Fangli, Wang Guansuo, Lü Xin'gang, et al. 2011. Drift characteristics of green macroalgae in the Yellow Sea in 2008 and 2010. Chinese Science Bulletin, 56(21): 2236–2242, doi: 10.1007/s11434-011-4551-7

Qiao Fangli, Xia Changshui, Shi Jianwei, et al. 2004. Seasonal variability of thermocline in the Yellow Sea. Chinese Journal of Ocean-

ology and Limnology, 22(3): 299–305, doi: 10.1007/BF02842563
Ren Shihe, Xie Jiping, Zhu Jiang. 2014. The roles of different mechanisms related to the tide-induced fronts in the Yellow Sea in summer. Advances in Atmospheric Sciences, 31(5): 1079–1089, doi: 10.1007/s00376-014-3236-y
Shi Jie, Liu Yi, Mao Xinyan, et al. 2017. Interannual variation of spring phytoplankton bloom and response to turbulent energy generated by atmospheric forcing in the central Southern Yellow Sea of China: satellite observations and numerical model study. Continental Shelf Research, 143: 257–270, doi: 10.1016/j.csr.2016.06.008
Simpson J H, Sharples J. 2012. Introduction to the Physical and Biological Oceanography of Shelf Seas. Cambridge: Cambridge University Press
Sun Jun, Feng Yuanyuan, Wang Dan, et al. 2013. Bottom-up control of phytoplankton growth in spring blooms in Central Yellow Sea, China. Deep Sea Research Part II: Topical Studies in Oceanography, 97: 61–71, doi: 10.1016/j.dsr2.2013.05.006
Sun Junchuan, Yang Dezhou, Yin Baoshu, et al. 2018. Onshore warm tongue and offshore cold tongue in the western Yellow Sea in winter: the evidence. Journal of Oceanology and Limnology, 36(5): 1475–1483, doi: 10.1007/s00343-018-7021-0
Tang Qisheng, Ying Yiping, Wu Qiang. 2016. The biomass yields and management challenges for the Yellow sea large marine ecosystem. Environmental Development, 17(S1): 175–181
Wang Baodong. 2000. Characteristics of variations and interrelations of biogenic elements in the Huanghai Sea Cold Water Mass. Haiyang Xuebao (in Chinese), 22(6): 47–54
Wang Xiaohua, Cho Y K, Guo Xinyu, et al. 2015a. The status of coastal oceanography in heavily impacted Yellow and East China Sea: past trends, progress, and possible futures. Estuarine, Coastal and Shelf Science, 163: 235–243, doi: 10.1016/j.ecss.2015.05.039
Wang Bin, Hirose N, Yuan Dongliang, et al. 2017. Effects of tides on the cross-isobath movement of the low-salinity plume in the western Yellow and East China Seas in winter. Continental Shelf Research, 143: 228–239, doi: 10.1016/j.csr.2016.06.011
Wang Fan, Liu Chuanyu, Meng Qingjia. 2012. Effect of the Yellow Sea warm current fronts on the westward shift of the Yellow Sea warm tongue in winter. Continental Shelf Research, 45: 98–107, doi: 10.1016/j.csr.2012.06.005
Wang Jia, Oey L Y. 2016. Seasonal exchanges of the Kuroshio and shelf waters and their impacts on the shelf currents of the East China Sea. Journal of Physical Oceanography, 46(5): 1615–1632, doi: 10.1175/JPO-D-15-0183.1
Wang Zongling, Xiao Jie, Fan Shiliang, et al. 2015b. Who made the world's largest green tide in China?—an integrated study on the initiation and early development of the green tide in Yellow Sea. Limnology and Oceanography, 60(4): 1105–1117, doi: 10.1002/lno.10083
Wei Qinsheng. 2016. Characteristics and mechanisms of chemical hydrology and ecological responses in the southern Yellow Sea and off the Changjiang Estuary (in Chinese) [dissertation]. Qingdao: Ocean University of China
Wei Qinsheng, Fu Mingzhu, Li Yan, et al. 2013a. Observation of the seasonal evolution of DO, Chlorophyll a maximum phenomena and nutrient accumulating in the southern Huanghai (Yellow) Sea Cold Water Mass area. Haiyang Xuebao (in Chinese), 35(4): 142–154
Wei Qinsheng, Li Xiansen, Wang Baodong, et al. 2016a. Seasonally chemical hydrology and ecological responses in frontal zone of the central southern Yellow Sea. Journal of Sea Research, 112: 1–12, doi: 10.1016/j.seares.2016.02.004
Wei Qinsheng, Liu Lu, Zhan Run, et al. 2010a. Distribution features of the chemical parameters in the Southern Yellow Sea in summer. Periodical of Ocean University of China (in Chinese), 40(1): 82–88
Wei Hao, Luo Xiaofan, Zhao Yiding, et al. 2015. Intraseasonal variation in the salinity of the Yellow and East China Seas in the summers of 2011, 2012, and 2013. Hydrobiologia, 754(1): 13–28, doi: 10.1007/s10750-014-2133-9
Wei Qinsheng, Lü Xingang, Wang Zongxing, et al. 2010b. A preliminary analysis of the characteristics of the continental shelf front and its ecological effects in the Yellow Sea. Advances in Earth Sciences (in Chinese), 25(4): 435–443
Wei Hao, Su Jilan, Wan Ruijing, et al. 2003. Tidal front and the convergence of anchovy (*Engraulis japonicus*) eggs in the Yellow Sea. Fisheries Oceanography, 12(4–5): 434–442, doi: 10.1046/j.1365-2419.2003.00259.x
Wei Qinsheng, Wang Huiwu, Ge Renfeng, et al. 2013b. Chemical hydrography and seasonal succession in the border between Yellow Sea and East China Sea. Oceanologia et Limnologia Sinica (in Chinese), 44(5): 1170–1181
Wei Qinsheng, Wang Huiwu, Ge Renfeng, et al. 2013c. Vertical distribution of suspended matter and implications in the southern Yellow Sea. Advances in Earth Sciences (in Chinese), 28(3): 374–390
Wei Hao, Wang Lei, Lin Yian, et al. 2002. Nutrient transport across the thermocline in the central Yellow Sea. Advances in Marine Science (in Chinese), 20(3): 15–20
Wei Qinsheng, Wang Baodong, Yao Qingzhen, et al. 2018. Hydrobiogeochemical processes and their implications for *Ulva prolifera* blooms and expansion in the world's largest green tide occurrence region (Yellow Sea, China). Science of the Total Environment, 645: 257–266, doi: 10.1016/j.scitotenv.2018.07.067
Wei Qinsheng, Wang Baodong, Yao Qingzhen, et al. 2019. Physical-biogeochemical interactions and potential effects on phytoplankton and *Ulva prolifera* in the coastal waters off Qingdao (Yellow Sea, China). Acta Oceanologica Sinica, 38(2): 11–23, doi: 10.1007/s13131-019-1344-3
Wei Qinsheng, Yu Zhigang, Ge Renfeng, et al. 2013d. Chemicohydrographic analysis of the role of the Yellow Sea western coastal cold water in forming the southern Yellow Sea western bottom cold water and its seasonal succession. Oceanologia et Limnologia Sinica (in Chinese), 44(4): 890–905
Wei Qinsheng, Yu Zhigang, Wang Baodong, et al. 2016b. Coupling of the spatial-temporal distributions of nutrients and physical conditions in the southern Yellow Sea. Journal of Marine Systems, 156: 30–45, doi: 10.1016/j.jmarsys.2015.12.001
Wei Qinsheng, Yu Zhigang, Wang Baodong, et al. 2017. Offshore detachment of the Changjiang River plume and its ecological impacts in summer. Journal of Oceanography, 73(3): 277–294, doi: 10.1007/s10872-016-0402-0
Wu Hui, Gu Jinghua, Zhu Ping. 2018. Winter counter-wind transport in the inner southwestern Yellow Sea. Journal of Geophysical Research, 123(1): 411–436, doi: 10.1002/2017JC013403
Wu Hui, Shen Jian, Zhu Jianrong, et al. 2014. Characteristics of the Changjiang plume and its extension along the Jiangsu Coast. Continental Shelf Research, 76: 108–123, doi: 10.1016/j.csr.2014.01.007
Wu Xiao, Xu Jingping, Wu Hui, et al. 2019. Synoptic variations of residual currents in the Huanghe (Yellow River)-derived distal mud patch off the Shandong Peninsula: implications for long-term sediment transport. Marine Geology, 417: 106014, doi: 10.1016/j.margeo.2019.106014
Xing Qianguo, An Deyu, Zheng Xiangyang, et al. 2019. Monitoring seaweed aquaculture in the Yellow Sea with multiple sensors for managing the disaster of macroalgal blooms. Remote Sensing of Environment, 231: 111279, doi: 10.1016/j.rse.2019.111279
Xiong Xuejun, Hu Xiaomin, Guo Yanliang, et al. 2019. Existence, morphology and structure of the Yellow Sea Warm Current Branch approaching waters offshore Qingdao, China. Science China Earth Sciences, 62(7): 1167–1180, doi: 10.1007/s11430-018-9331-1
Yu Fei, Zhang Zhixin, Diao Xinyuan, et al. 2006. Analysis of evolution of the Huanghai Sea Cold Water Mass and its relationship with adjacent water masses. Haiyang Xuebao (in Chinese), 28(5): 26–34
Yuan Dongliang, Hsueh Y. 2010. Dynamics of the cross-shelf circulation in the Yellow and East China Seas in winter. Deep Sea Research Part II: Topical Studies in Oceanography, 57(19–20): 1745–1761, doi: 10.1016/j.dsr2.2010.04.002
Yuan Dongliang, Li Yao, Wang Bin, et al. 2017. Coastal circulation in

the southwestern Yellow Sea in the summers of 2008 and 2009. Continental Shelf Research, 143: 101–117, doi: 10.1016/j.csr.2017.01.022

Yuan Chengyi, Wang Yuheng, Wei Hao. 2014. Estimating the budgets of nutrients for phytoplankton bloom in the central Yellow Sea using a modified lower tropic ecosystem model. Journal of Ocean University of China, 13(1): 1–12, doi: 10.1007/s11802-014-1900-6

Yuan Dongliang, Zhu Jianrong, Li Chunyan, et al. 2008. Cross-shelf circulation in the Yellow and East China Seas indicated by MODIS satellite observations. Journal of Marine Systems, 70(1–2): 134–149, doi: 10.1016/j.jmarsys.2007.04.002

Zhai Weidong. 2018. Exploring seasonal acidification in the Yellow Sea. Science China Earth Sciences, 61(6): 647–658, doi: 10.1007/s11430-017-9151-4

Zhang Zhixin. 2014. Observation and analysis of the coastal current and its adjacent current system in the China offshore waters (in Chinese) [dissertation]. Qingdao: Ocean University of China

Zhang Shuwen, Wang Qingye, Lü Yan, et al. 2008. Observation of the seasonal evolution of the Yellow Sea Cold Water Mass in 1996–1998. Continental Shelf Research, 28(3): 442–457, doi: 10.1016/j.csr.2007.10.002

Zhao Baoren. 1985. The fronts of the Huanghai Sea Cold Water Mass induced by tidal mixing. Oceanologia et Limnologia Sinica (in Chinese), 16(6): 451–460

Zhao Baoren. 1987. A preliminary study of continental shelf fronts in the western part of southern Huanghai Sea and circulation structure in the front region of the Huanghai Cold Water Mass (HCWM). Oceanologia et Limnologia Sinica (in Chinese), 18(3): 218–226

Zhao Sheng, Yu Fei, Diao Xinyuan, et al. 2011. The path and mechanism of the Yellow Sea Warm Current. Marine Sciences (in Chinese), 35(11): 73–80

Zhou Feng, Huang Daji, Wan Ruijing, et al. 2008. Observations and analysis of tidal fronts in the southwestern Huanghai Sea. Haiyang Xuebao (in Chinese), 30(3): 9–15

Zhou Mingjiang, Liu Dongyan, Anderson D M, et al. 2015. Introduction to the special issue on green tides in the Yellow Sea. Estuarine, Coastal and Shelf Science, 163: 3–8, doi: 10.1016/j.ecss.2015.06.023

Zhou Feng, Xuan Jiliang, Huang Daji, et al. 2013. The timing and the magnitude of spring phytoplankton blooms and their relationship with physical forcing in the central Yellow Sea in 2009. Deep Sea Research Part II: Topical Studies in Oceanography, 97: 4–15, doi: 10.1016/j.dsr2.2013.05.001

Zhu Ping, Wu Hui. 2018. Origins and transports of the low-salinity coastal water in the southwestern Yellow Sea. Acta Oceanologica Sinica, 37(4): 1–11, doi: 10.1007/s13131-018-1200-x